Supporting Information

Development of O_2 and NO co-doped porous carbon as high capacity mercury sorbent

Fenghua Shen, Jing Liu,* Dawei Wu, Yuchen Dong, Zhen Zhang

State Key Laboratory of Coal Combustion, School of Energy and Power Engineering, Huazhong University of Science and Technology, Wuhan 430074, China

Number of pages: 12

Number of figures: 7

Number of tables: 1

* Corresponding author. Tel.: 86-27-87545526

E-mail address: liujing27@mail.hust.edu.cn (J. liu)

Computational Details

All of the calculations were performed by applying Gaussian 09 software package.[1] Density functional theory (DFT) has been employed, and full geometric optimizations and energy calculations were performed at B3PW91 level of theory. Effective core potential (ECP) was used to replace inner electrons of Hg, as a result of the large amount of electrons in heavy elements. It has been validated that the B3PW91/RCEP60VDZ combination can provide reasonably accurate results comparing to experimental data.[2,3] Therefore, B3PW91/RCEP60VDZ was employed for the Hg atom in this study. The 6-31G(d) basis set was used for non-metal elements (C, O, N and H).

The total adsorption energy can be calculated as the following equation:

$$E_{ads} = E(AB) - (E(A)+E(B))$$

where E(A) is the energy of the adsorbate, E(B) is the energy of the porous carbon surface, and E(AB) is the total energy of the whole adsorption system.

Solid-state ^{13}C NMR characterization experimental data showed that carbon had chemical structures consisting of 3-7 benzene rings.[4] It was found that the reactivity of the active sites strongly depended on its local shape rather than on the size of the cluster models.[5,6] Therefore, a single graphite layer (seven-ring zigzag: $C_{25}H_9$) cluster model was used to simulate the porous carbon (PC) surface. The upper side carbon atoms in this model were unsaturated to simulate the active sites and the carbon atoms on the other sides were terminated with hydrogen atoms. The optimized bond lengths (average C-C: 1.41 Å, C-H: 1.09 Å) and bond angles (average ∠C-C-C: 121°, ∠C-C-H: 120°) were obtained for this cluster model, which were in good agreement with the experimental data (C-C: 1.42 Å, C-H: 1.07 Å, ∠C-C-C: 120°, ∠C-C-H: 120°).[5]

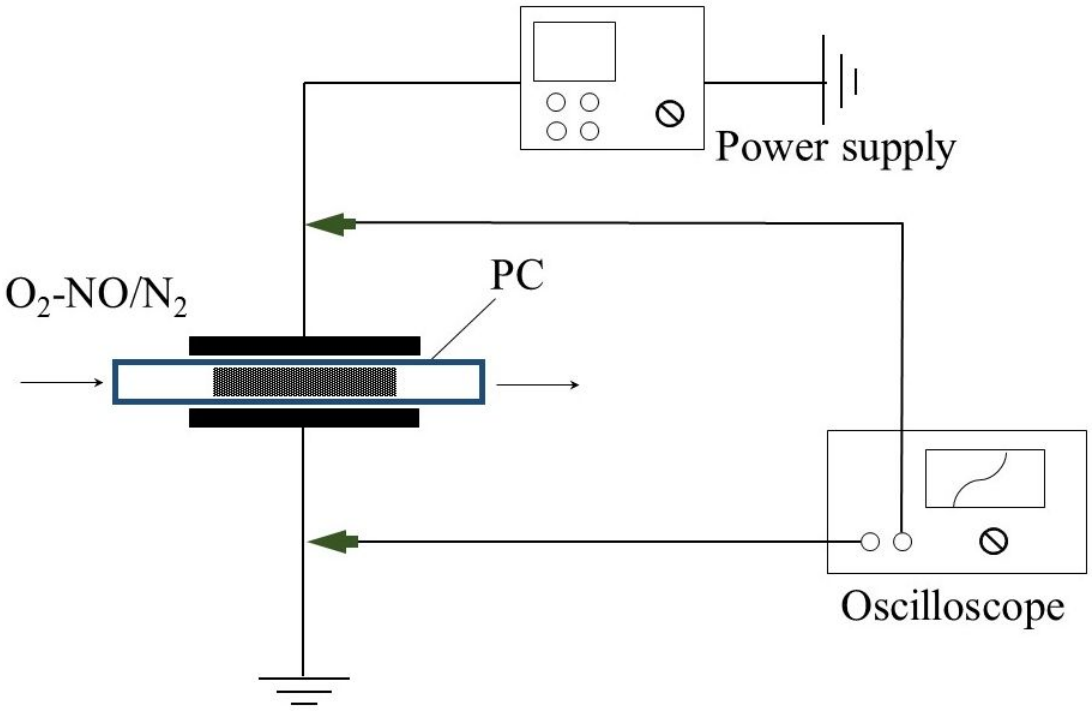

Figure S1. Non-thermal plasma treatment setup

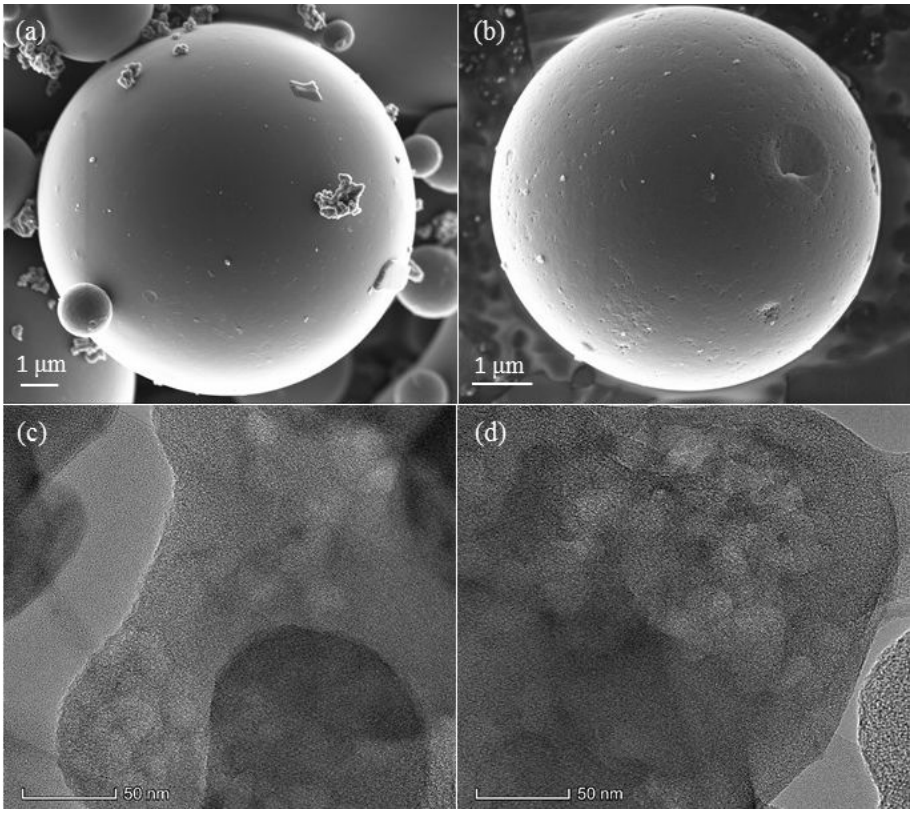

Figure S2. SEM images of (a) PC and (b) PC-O4N2T3; TEM images of (c) PC and (d) PC-O4N2T3.

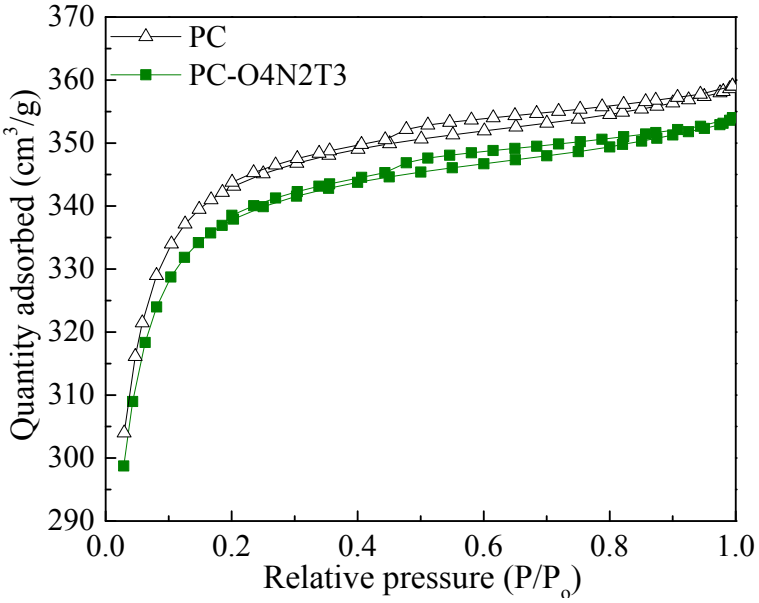

Figure S3. Nitrogen adsorption-desorption isotherms of PC and PC-O4N2T3.

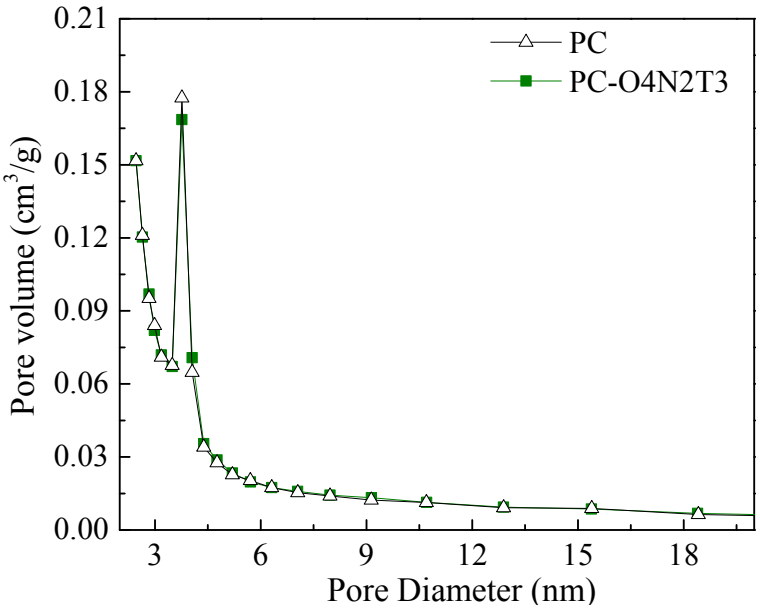

Figure S4. Pore size distributions of PC and PC-O4N2T3.

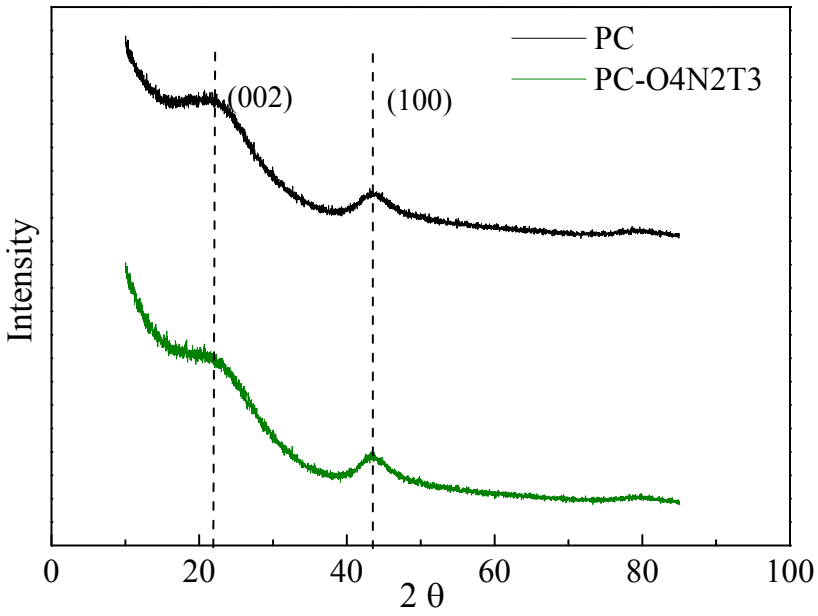

Figure S5. XRD patterns of PC and PC-O4N2T3.

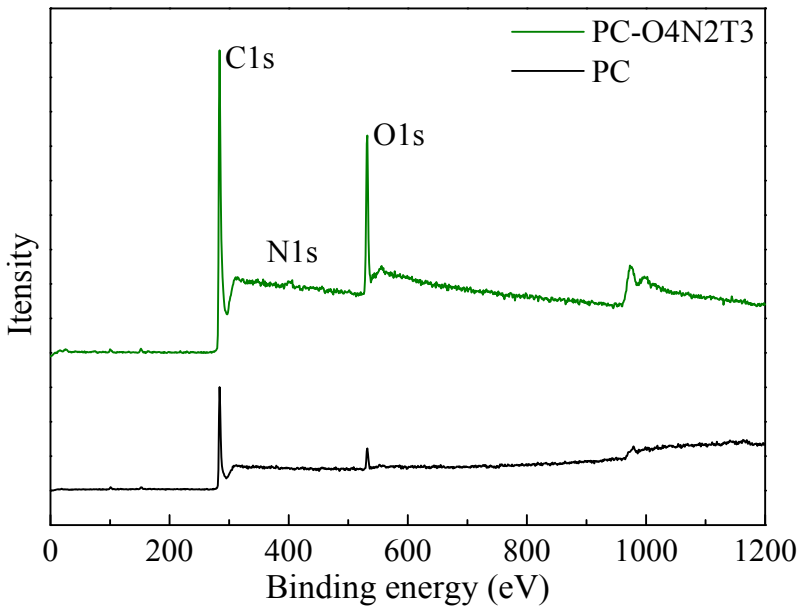

Figure S6. XPS spectra of PC and PC-O4N2T3

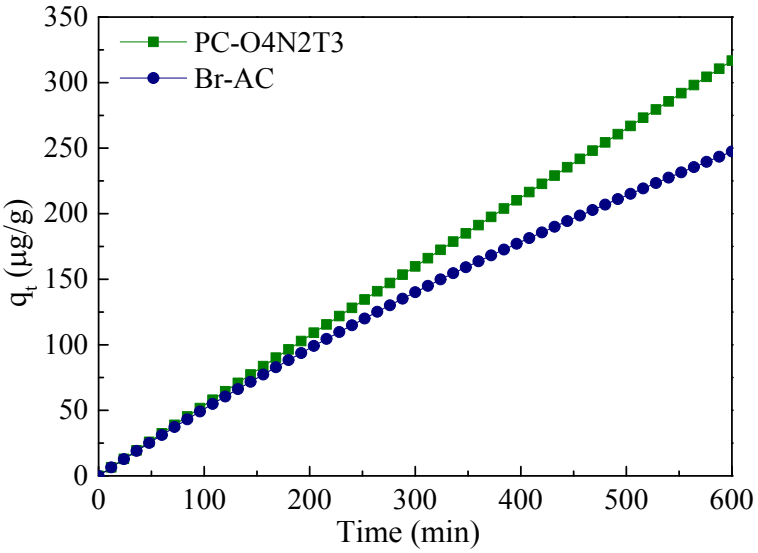

Figure S7. Simulation of Hg^0 adsorption by pseudo-second-order model.

Table S1. Kinetic parameters of the pseudo-second-order model for PC-O4N2T3 and Br-AC

	k (g/(μg·min))	q_e (μg/g)	R^2
PC-O4N2T3	3.57E-09	12315	0.97
Br-AC	4.76E-07	1061	0.99

References

(1) Frisch, M.; Trucks, G.; Schlegel, H.; Scuseria, G.; Robb, M.; Cheeseman, J.; Scalmani, G.; Barone, V.; Mennucci, B.; Petersson, G.; Nakatsuji, H.; Caricato, M.; Li, X.; Hratchian, H.; Izmaylov, A.; Bloino, J.; Zheng, G.; Sonnenberg, J.; Hada, M.; Ehara, M.; Toyota, K.; Fukuda, R.; Hasegawa, J.; Ishida, M.; Nakajima, T.; Honda, V.; Kitao, O.; Nakai, H.; Vreven, T.; Montgomery, J.; Peralta, J.; Ogliaro, F.; M. Bearpark, M.; Heyd, J.; E. Brothers, E.; Kudin, K.; Staroverov, V.; Kobayashi, R.; Normand, J.; Raghavachari, K.; Rendell, A.; Burant, J.; Iyengar, S.; Tomasi, J.; Cossi, M.; Rega, N.; Millam, J.; Klene, M.; Knox, J.; Cross, J.; Bakken, V.; Adamo, C.; Jaramillo, J.; Gomperts, R.; Stratmann, R.; Yazyev, O.; Austin, A.; Cammi, R.; Pomelli, C.; Ochterski, J.; Martin, R.; Morokuma, K.; Zakrzewski, V.; Voth, G.; Salvador, P.; JDannenberg, J.; Dapprich, S.; Daniels, A.; Farkas, O.; Foresman, J.; Ortiz, J.; Cioslowski, J.; Fox, D., Gaussian 09, ReVisions D.01. Gaussian, Inc., Wallingford CT **2009**.

(2) Liu, J.; Qu, W.; Yuan, J.; Wang, S.; Qiu, J.; Zheng, C., Theoretical studies of properties and reactions involving mercury species present in combustion flue gases. *Energ. Fuel* **2010,** *24*, (1), 117-122.

(3) Liu, J.; Cheney, M. A.; Wu, F.; Li, M., Effects of chemical functional groups on elemental mercury adsorption on carbonaceous surfaces. *J. Hazard. Mater.* **2011,** *186*, (1), 108-113.

(4) Perry, S.; Hambly, E.; Fletcher, T.; Solum, M.; Pugmire, R., Solid-state ^{13}C NMR characterization of matched tars and chars from rapid coal devolatilization. *P. Combust. Inst.* **2000,** *28*, (2), 2313-2319.

(5) Chen, N.; Yang, R. T., Ab initio molecular orbital calculation on graphite: selection of molecular system and model chemistry. *Carbon* **1998,** *36*, 1061-1070.

(6) Montoya, A.; Truong, T.-T. T.; Mondragón, F.; Truong, T. N., CO Desorption from oxygen species on carbonaceous surface: 1. Effects of the local structure of the active site and the surface coverage. *J. Phys. Chem. A* **2001,** *105*, 6757-6764.